β-(1→3)(1→6) glucan from *Schizophyllum commune* 227E.32: high yield production via glucose/xylose co-metabolization

Ana Paula Vanin[a*], Esther Ziliotto Visentin[a], Roselei Claudete Fontana[a], Maria Carolina Bezerra di Medeiros Leal[b], Scheila de Avila e Silva[c] Bjørn Torger Stokke[d], Elaine Rosechrer Carbonero[e], Marli Camassola[a]

[a] Enzymes and Biomass Laboratory, Institute of Biotechnology, University of Caxias do Sul, Caxias do Sul, RS, Brazil.

[b] Nuclear Magnetic Resonance Laboratory, Federal University of São Carlos, São Carlos, SP, Brazil

[c] Computational Biology and Bioinformatics Laboratory, Bioinformatics Research Center, Institute of Biotechnology, University of Caxias do Sul, Caxias do Sul, RS, Brazil.

[d] Biophysics and Medical Technology, Department of Physics, NTNU Norwegian University of Science and Technology, Trondheim, Norway.

[e] Institute of Chemistry, Federal University of Catalão, Catalão, GO, Brazil.

[*] Corresponding author

Abstract

A co-metabolization of xylose and glucose by *Schizophyllum commune* 227E.32 wild mushroom for exopolysaccharide (EPS) production is presented. Experiments were conducted to evaluate the EPS production in a culture medium supplemented with four xylose concentrations (20, 50, 100 and 150 $g.L^{-1}$). A xylose concentration of 50 $g.L^{-1}$ yielded the best EPS production, 4.46 $g.L^{-1}$. The scale-up in a stirred tank reactor (STR)

was performed. The strain produced 1.82 $g.L^{-1}$ and 2.03 $g.L^{-1}$ EPS with 10% and 20% pre-inoculum, respectively. It was possible to demonstrate the ability of this strain to metabolize a pentose as a carbon source. Purification steps were conducted with the EPS, and GC-MS analysis showed a monosaccharide composition of 100% glucose. ^{13}C NMR and HSQC-edited showed that the EPS to consists of a β-D-Glcp (1→3) main chain, partially substituted at O-6 with non-reducing β-D-Glcp ends on every third residue. The M_w of the EPS was determined by GPC to 1.5 x 10^6 $g.mol^{-1}$ (shaken flasks) and 1.1 x 10^6 $g.mol^{-1}$ (STR fermentation). AFM topographs revealed a semi-flexible appearance of the EPS that is consistent with the triple helical structures adopted by such EPS, and overall contour length consistent with a high molar mass.

Keywords: xylose/glucose pathway, schizophyllan, exopolysaccharides, betaglucan.

1. Introduction

Macrofungi are a large and diverse phylum of fungi, popularly known as mushrooms. In recent years, they have been extensively studied for various value-added and industrial interest products, such as enzymes, extracts, and polysaccharides (Rekik et al., 2019; Schneider et al., 2020)

β-D-glucans are a group of polysaccharides that can be extracted from different sources: cereals such as oat (Nguyen et al., 2021), bacteria (Utama et al., 2021), from fungi such as yeasts (Ruiz-Herrera & Ortiz-Castellanos, 2019)and mushrooms (Carbonero et al., 2012), for example. Concerning metabolites produced by mushrooms, the exopolysaccharides (EPS) for medical and pharmaceutical applications stand out (Liu et al., 2019; Zhang et al., 2018). Some of these EPS are β-D-glucans consisting of monomeric units of D-glucose linked through by β-(1→3) glycosidic bonds, with or without branched β-(1→6)-D-glucose units. They have been produced in liquid cultures or extracted from mycelium (Zhu et al., 2016). Some fungal β-D-glucans are well-known

and studied as reported in the literature, such as lentinan from *Lentinula edodes* (Xu et al., 2016), scleroglucan from *Sclerotium rolfsii* (Fariña et al., 2001; Viñarta et al., 2007) and schizophyllan (SPG) from *Schizophyllum commune* (Jamshidian et al., 2016). SPG is a water-soluble β-glucan. It was first extracted from the mycelium of the fungus *Schizophyllum commune* and then it was produced as an exopolysaccharide from submerged cultures. SPG consists of a β-(1→3)-D-glucose backbone with a single β-(1→6)-linked glucose side chain on every third residue (Zhang et al., 2013). SPG has been widely reported because of its application in various fields of science and industrial processes. Some of them are immune properties (Smirnou et al., 2017); intestinal anti-inflammatory effects (Du et al., 2017); antitumor activity (Zhong et al., 2015); SPG-based nanogels for drug delivery (Zhang et al., 2013); enhanced oil recovery (Shoaib et al., 2020); nanofibers for wound healing (Safaee-Ardakani et al., 2019); hybrid nanogels for topical dermal delivery (Kim et al., 2021); antiaging, lifting and hydrating agent lotions (Wu et al., 2016).

Previous studies have reported SPG production with glucose or other hexoses as carbon sources, through submerged cultures of *S. commune* strains, in bioreactors or shaken flasks (Leathers et al., 2016). *S. commune* is well-known for having a lignolytic enzymes apparatus capable of degrading woody cell-wall components, including cellulose and hemicellulose, which are rich in glucose and xylose, respectively. Some researchers are exploring alternative substrates, cheaper and environmental appeal substitutes, like agricultural wastes (Singh et al., 2017; Sutivisedsak et al., 2013). As far as we know, only one work investigated the production of SPG using xylose as a single carbon source (Shu & Hsu, 2011), but that work did not extend to elucidate the pentose metabolic pathway. Nevertheless, the mechanisms of pentose metabolization by

mushrooms still need to be fully understood. A better knowledge of this process could help to optimize the production process and use different carbon resources.

This study aimed to select one macrofungus from eight wild isolated strains to EPS production, using three carbon sources. The EPS produced was then isolated and characterized.

2. Materials and Methods

2.1 Macrofungi strains

Eight macrofungi strains from the Enzymes and Biomasses Laboratory, isolated from the Atlantic Forest biome, were selected for a first screening: *Lentinus crinitus* 20M_SE and 154L21_SE, *Trametes villosa* 43HA, *Schizophyllum commune* 227E.32 and VE_07, *Bjerkandera fumosa* 29H, *Auricularia fuscosuccinea* 78F3, *Pycnoporus sanguineus* 14G. These strains were grown on potato dextrose agar plates, 28°C, for 12 days.

2.2 Screening of macrofungi strains in shaken flasks

This work employed a semi synthetic culture medium (SSC) in all submerged cultures. SSC consisted of a potato broth at 200 $g.L^{-1}$ (Schneider et al., 2020) supplemented with 50 $mL.L^{-1}$ of a salt solution (Mandels & Reese, 1960). The submerged cultures were performed with SSC medium supplemented with 20 $g.L^{-1}$ xylose, 20 $g.L^{-1}$ sucrose, and 20 $g.L^{-1}$ glucose. The experiments were carried out in 500 mL Erlenmeyer flasks, 100 mL total volume. Flasks were sterilized in an autoclave (1.05 bar, 121°C, 15 min) and inoculated with three 1.5 cm discs of each strain. The flasks were placed in triplicate on a reciprocal shaker (150 rpm), controlled temperature (28°C) for 288 hours. Three flasks were collected every 48 hours from each strain.

2.3 EPS production by *S. commune* 227E.32 in shaken flasks

A 96-hour pre-inoculum was prepared with SSC medium supplemented with 20 $g.L^{-1}$ glucose. The pre-inoculum was incubated on a reciprocal shaker at 150 rpm, 28°C. Subsequently, a screening was performed with four concentrations of xylose (20, 50, 100 and 150 $g.L^{-1}$) and 10% (v/v) of pre-inoculum. The experiments were carried out on a reciprocal shaker for 216 hours, at 28°C, 150 rpm, in triplicate. Three flasks were collected every 24 hours.

2.4 Scale-up of EPS production from *S. commune* 227E.23 in a STR

Two experiments were performed in a 10L STR (New Brunswick, BioFlo®/Celligen® 115), 5L working volume. A 96-hour pre-inoculum was prepared under the conditions as described in the 2.3 section. STR's with SSC medium were inoculated with 10% (v/v) and 20% (v/v) of the pre-inoculum. As a complementary carbon source, 50 $g.L^{-1}$ of xylose was added. The operating conditions of these experiments were: operating temperature, 28°C; gas flow, 0.5 vvm; stirring speed, 200-450 rpm; initial pH 5.00 (uncontrolled); 336 hours.

2.5 Viscosity measurements

The culture broth was separated from the macrofungus mycelium by centrifugation at 14000 g, 30 min, and 4 °C (Eppendorf 5810 R). The viscosity measurements were performed with 50 mL of broth on a Brookfield DV-I Prime Digital Viscometer (spindles LV1 and LV2). The samples were maintained in a recirculating bath at 25 °C and stabilized for two minutes before to the viscosity reading.

2.6 Analytical determinations

The mycelium, previously separated by centrifugation, was oven dried (60°C) on a previously weighed filter paper. Glucose, sucrose, xylose, xylitol, and ethanol were

119 analyzed using high performance liquid chromatography (HPLC, Shimadzu), with an
120 Aminex HPX-87H column (Bio-Rad®) at 60 °C, mobile phase H_2SO_4 5 mmol.L^{-1}, flow
121 rate of 0.6 mL.min^{-1}. Sucrose was quantified using acid hydrolysis with HCl , according
122 to (Falcone & Marques, 1965).

123 **2.7 Isolation and purification of β-(1,3)(1,6) glucan produced by *S. commune***

124 The EPS produced and secreted into the culture broth by *S. commune* 227E.32 was
125 recovered by the addition of 96% ethanol (1:1) and stored in a freezer overnight for its
126 complete precipitation, according to the methodology described by (Fariña et al., 2001).
127 The precipitate was collected from the ethanol mixture with a fine sieve, centrifuged to
128 remove excess ethanol, freeze-dried, and grounded in a coffee grinder (Oster, model
129 OMDR100, 60 Hz, 220V) until a fine light brown powder was obtained. Afterwards,
130 purification steps were performed to isolate the β-(1,3)(1,6) glucan from EPS crude
131 material, as shown in Fig. 1.

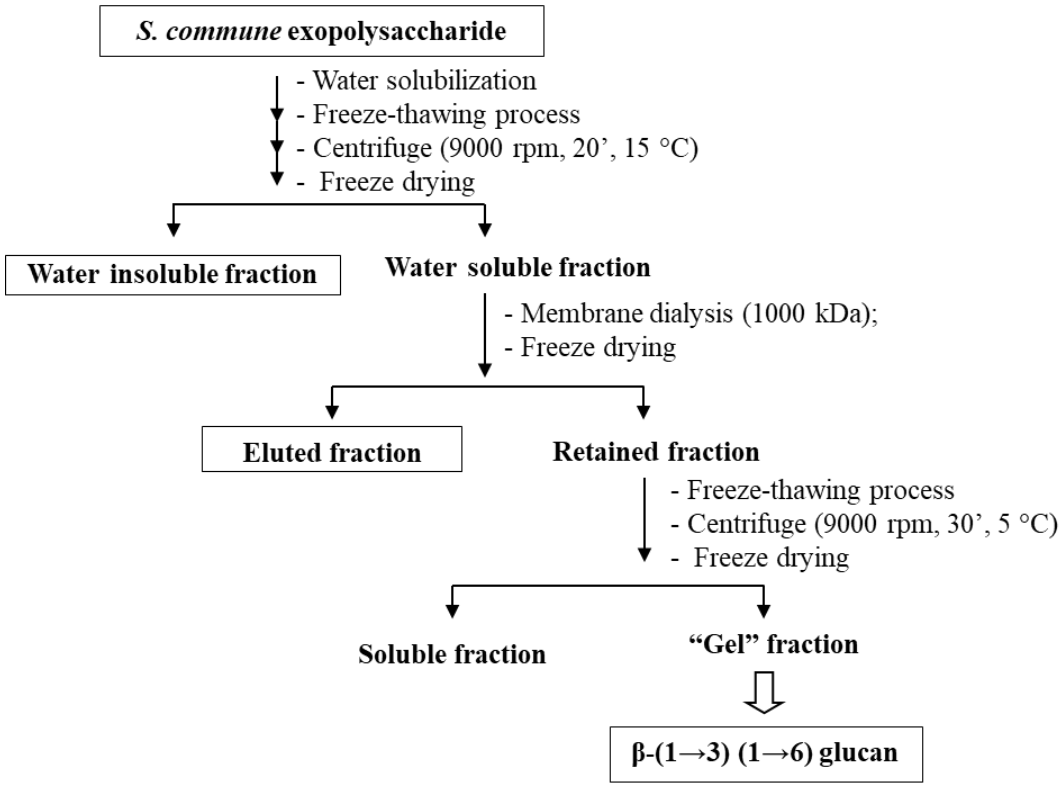

Fig. 1. Purification flowchart of a β-(1,3)(1,6) glucan produced by the *S. commune* 227E.32 strain in an STR.

2.8 Monosaccharide compositions

Monosaccharide compositions of the fractions from EPS purification steps were determined by Gas Chromatography Coupled with Mass Spectrometry (GC-MS) after monosaccharides conversion to alditol acetates (Wolfrom & Thompsom, 1963; Wolfrom & Thompson, 1963). The products obtained were solubilized in acetone, analyzed in GC-MS and identified by retention time and mass fragment profile.

2.9 Polysaccharide methylation

The purified fraction (EXO-MR "gel") was methylated according to the method previously described by Ciucanu & Kerek, 1984. The methylated derivatives were analyzed as partially methylated alditol acetates by GC-MS, and identified through retention time and mass fragmentation, which were confirmed by comparison with the spectral database of the Complex Carbohydrate Research Center (CCRC;

147 https://glygen.ccrc.uga.edu/ccrc/databases/index.php). The results were expressed as the
148 relative percentage of each derivative.

149 **2.10 Gas Chromatography coupled with Mass Spectrometry (GC-MS)**

150 The GC-MS was performed using an Agilent Technologies gas chromatograph,
151 model 7820A, coupled to an Agilent 5975E mass spectrometer equipped with an HP5-
152 MS fused silica capillary column (0.25 mm x 30 m x 0.25 µm), with an electron impact
153 ionization source (70 eV) and an Ion Trap type analyzer. Data processing was performed
154 in the Data Analysis software.

155 **2.11 Nuclear magnetic resonance spectroscopy (NMR)**

156 NMR spectra were performed in a Bruker spectrometer, model Avance III, 9.4
157 Tesla (400 MHz for hydrogen frequency). Heteronuclear Single Quantum Coherence-
158 Editing (HSQC-edit) analyzes were performed at 50 ºC, and ^{13}C NMR at 70°C. The
159 polysaccharide fraction (~ 30 mg) was solubilized in deuterated dimethylsulfoxide
160 (Me_2SO-d_6). Chemical shifts were expressed in ppm (δ), in accordance with the ^{1}H (δ 2.5)
161 and ^{13}C (δ 39.7) signals of the solvent utilized. NMR spectra were processed in Bruker's
162 TopSpin™ software, version 3.6.3.

163 **2.12 Atomic Force Microscopy (AFM)**

164 The EPS specimens for AFM imaging were prepared using the deposition of diluted
165 solutions in glycerol on mica and subsequent vacuum drying as outlined by Tyler &
166 Branton, 1980. A stock solution of isolated the β-(1,3)(1,6)glucan (1 mg. mL^{-1}) was
167 prepared by initially dissolving an appropriate amount of the purified polysaccharide in
168 MQ-water. The solution was stirred overnight (about 16 hours) at room temperature (25
169 °C) to ensure complete solubilization. Afterwards, dilutions (1-20 µg. mL^{-1}) of the stock
170 solution were prepared in 60% (v/v) glycerol solution. 75 µL of the diluted solutions were

sprayed on freshly cleaved mica discs and left to dry in vacuum at $1.3x10^{-3}$ Pa or lower for about 14 hours. β-glucan AFM topographs were obtained using a Digital Instruments Multi-mode IIIa atomic force microscope equipped with an E-scanner. Silicon nitride cantilevers (PPP-NCH-W, Pointprobe plus, Nanosensors), nominal spring constants (10–130 N/m), and nominal resonance frequencies (200–500 kHz). The range of scan sizes were 1x1 µm up to 7x7 µm and scanning rates up to 2.5 Hz. The instrument was operated in tapping mode as described previously by Stokke et al., 2001. The topographs (512 x 512 pixels up to 992 x 992 pixels) were flattened in the AFM software.

2.13 Determination of homogeneity of glucans and their molecular weight

The homogeneity and weight average molar mass (M_w) of the β-glucans were analyzed with an Agilent 1260 Infinity II Multi GPC-SEC System, using Refractive Index (RID), Ultraviolet (UV), and Dual Angle Light Scattering (LSD) detectors. The separation was done on an Agilent PL Aquagel-OH MIXED-H column (300 × 7.5 mm, 8 µm) at a constant temperature of 30 °C. The injection volume was 100 µL. The mobile phase was 0.1 M $NaNO_2$ with 0.2 $g.L^{-1}$ sodium azide and a flow rate of 1.0 $mL.min^{-1}$. The samples (1 $mg.ml^{-1}$) were solubilized in the eluent solution and filtered through 0.22 µm pore size membranes. The molecular weight was calculated using a calibration curve generated from dextran standards. Data were acquired and analyzed using Agilent GPC/SEC software (Agilent Technologies, Cheadle, United Kingdom).

2.14 Statistics, illustrations and graphics

All statistics were performed in Statistica 10.0 software. Data were expressed as means and standard deviations of triplicate experiments. The normality test ($p < 0.05$), Pearson's and Spearman's correlations were also used to compare and analyze the results

in shaken flasks. Illustrations were constructed by the authors in BioRender software. Graphics were plotted in Origin software.

3. Results and Discussion

3.1 Screening of macrofungi strains

Eight strains of macrofungi were selected for EPS production on three carbon sources: glucose, sucrose, and xylose. Increased viscosity of the culture broth indicates EPS production, especially when β-glucans are present (García-Ochoa et al., 2000). For this reason, in this first phase, the viscosity of the culture broths was evaluated (Fig. ***2***). pH, sugar consumption and mycelial growth were also measured, and these results are displayed in the supplementary material (Fig. S1).

The culture broth containing xylose as carbon source showed the highest viscosity compared to the other broths supplemented with glucose and sucrose. The culture broths of *S. commune* 227E.32 and *S. commune* VE07 strains (Fig. 3c) reached maximum values of viscosity between 192 and 288 hours of cultivation, when compared to the other strains (Fig 2a and 2b) in the same interval of time. However, the broth of *S. commune* 227E.32 grown with xylose reached higher viscosity, with values around 900 cP at 288 hours of cultivation. This result suggested that xylose may be an alternative supplementary substrate for EPS production. For this reason, *S. commune* 227E.32 was chosen to proceed with the next optimization and scale-up experiments with xylose as a complementary carbon source.

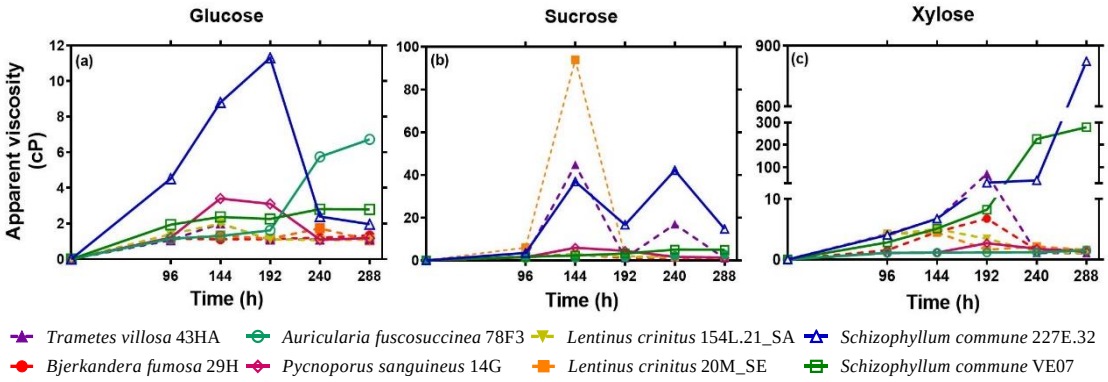

Fig. 2. Apparent viscosity of eight macrofungi strains cultivated in shaken flasks using 20 g.L^{-1} (a) glucose, (b) sucrose and (c) xylose as carbon sources.

3.2 Optimization of the EPS production by *S. commune* 227E.32 strain in shaken flasks

Mycelial growth, EPS production, and glucose/xylose concentration were analyzed with four xylose concentrations: 20, 50, 100, and 150 g.L^{-1} (Figure 3a and b). Pearson and Spearman's correlations are showed in Table S1 (supplementary material). Concentrations of 50, 100 and 150 g.L^{-1} had a similar mycelial growth profile until 216 hours of the experiment (Fig. 3a). Although cultivation time exerted a strong and proportional correlation regarding EPS production at all xylose concentrations, the strongest correlation was observed for 50 g.L^{-1} (0.965) of xylose. However, when EPS production was compared with mycelial growth, a strong (0.980) and medium (0.886) correlation was observed for the experiments with 50 g.L^{-1} and 100 g.L^{-1} of xylose, respectively. The same was not observed for 20 and 150 g.L^{-1} of xylose. EPS production with 50 g.L^{-1} and 100 g.L^{-1} xylose showed an inverse correlation with the consumption of glucose present in the culture medium. However it did not have the same correlation with xylose consumption.

The concentration of xylose and glucose (Fig. 3b) decreases proportionally until 216 hours for all experiments. *S. commune* 227E.32 not only had the ability to metabolize xylose in the presence of glucose but also had a specific regulatory mechanism between

these two carbon sources. The glucose and xylose pathway are illustrated in Figure 3. This behavior is indeed expected by this macrofungus genus, which was corroborated by Horisawa et al. (2015). They demonstrated that a *S. commune* strain could metabolize all xylose from the culture medium in 20 days of cultivation.

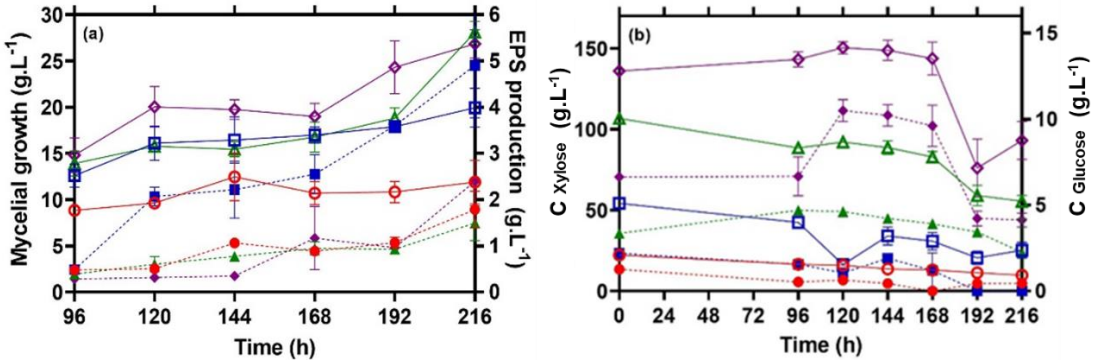

Figure 3. Mycelial growth and EPS production (a) and of xylose/glucose concentrations (b) by *S. commune* 227E.32 in shaken flasks. Purple, green, blue, and red lines:150 g. L^{-1}, 100 g. L^{-1}, 50 g. L^{-1}, 20 g. L^{-1}, respectively. Dashed lines: EPS production and glucose concentration. Continuous lines: mycelial growth and xylose concentration.

In this work, the media enriched with 50 $g.L^{-1}$ of xylose reached a higher amount of EPS, 4.46 $g.L^{-1}$, following 216 hours of the experiment. For this reason, this condition was chosen to proceed with scale-up experiments. Singh and collaborators (2017) have produced a closer value, 4.2 $g.L^{-1}$ but in 432 hours in a medium containing *Leucaena leucocephala* wood 2% (w/v), supplemented with 20 $g.L^{-1}$ of glucose. In contrast, another study with *S. commune* ATCC 38548 strain produced only 0.61 and 0.68 $g.L^{-1}$ of EPS in a medium containing pure glucose and xylose, respectively (Shu & Hsu, 2011). Other media containing wheat bran, malt waste and bagasse rich in glucose and xylose were studied by Jamshidian et al, (2016). These media had high concentrations of xylose coming from the biomasses, but the one with the highest amounts of glucose, wheat bran, produced the highest quantities of EPS, 2 $g.L^{-1}$. It seems that the strains could metabolize the carbon sources, but the mechanism through it is not explored and explained. This

mechanism of glucose/xylose consumption was closely explored in this work in the scale-up experiments as described in the following.

3.3 Scale-up of EPS production in an STR

Time course data of *S. commune* 227E.32 for EPS production, mycelial growth, xylose/glucose concentrations, xylitol, and ethanol productions in STR were evaluated (Fig 4 and Table 1). Experiment 1 (10% pre-inoculum) and Experiment 2 (20% pre-inoculum) were tested. Differences between specific EPS product yield ($Y_{P/X}$), product yield ($Y_{P/S}$) and mycelia yield ($Y_{X/S}$) were observed. Mycelial growth (X) (Fig 4a), increased from 24.70 up to 29.83 $g.L^{-1}$ in Experiment 2, and $Y_{X/S}$ increased considerably as well, from 8 to 14.21 g/g^{-1}. Experiment 2 showed superior values than Experiment 1 for EPS production (P), 2.03 $g.L^{-1}$ and $Y_{P/X}$, 0.082 $g.g^{-1}$, but not for $Y_{P/S}$, 0.66 $g.g^{-1}$. Although the optimal EPS production was reached by Experiment 2, the best $Y_{P/S}$ were obtained with Experiment 1, 0.90 $g.g^{-1}$. These observations led to the conclusion that Experiment 1 had the highest cost benefit ratio of sugar conversion into EPS.

Regarding glucose and xylose concentrations (Fig. 4b), *S. commune* 227E.32 has consumed both carbon sources concomitantly, although showing its preference for glucose. Experiment 1 had a higher consumption of glucose and xylose (75% and 40%, respectively) than Experiment 2 (72% and 27%, respectively). These results indicate that *S. commune* 227E.32 could metabolize glucose and xylose. Despite these experimental observations, to be more reports in the literature that explains the metabolic pathway of pentoses by mushrooms. However, several studies on wild and genetically modified yeasts for pentose metabolization can enlighten the understanding of this matter (Lee et al., 2020). Although *S. commune* 227E.32, which is studied in this work, has not been sequenced yet, gene sequences of other species strains are available in databases, such as the Kyoto Encyclopedia of Genes and Genomes - KEGG (https://www.genome.jp/kegg/).

Sequences for the genes for xylose reductase (SCHCODRAFT_13604) and xylulokinase (SCHCODRAFT_77105 and SCHCODRAFT_76089) were detected. This information could support the elucidation of the metabolic pathway of hexoses and pentoses proposed in Fig. 5. It is known that there are two xylose transport systems in fungal cell wall: a facilitated import system that can be shared by xylose/glucose, and a high-affinity xylose-proton system called H^+ sym (Chu & Lee, 2007; Matsushika et al., 2009). Once in the cytosol, xylose can undergo a series of biochemical reactions. It is suggested that these two metabolic pathways occurred concomitantly, and this observation could be concluded by xylitol and ethanol productions in both experiments (Fig. 4c). Ethanol was produced only at the end of fermentation in Experiment 1. In contrast, in Experiment 2, its production oscillates throughout the fermentation. Experiment 1 had 10% of initial pre-inoculum, with a smaller number of cells and well oxygen transfer, so it is suggested that the strain preferred to use available sugars for glycolysis and cell growth. The opposite was observed in Experiment 2. Because of low airflow, oxygen transfer was impaired causing a specific “anaerobic environment” for some cells leading to higher ethanol production.

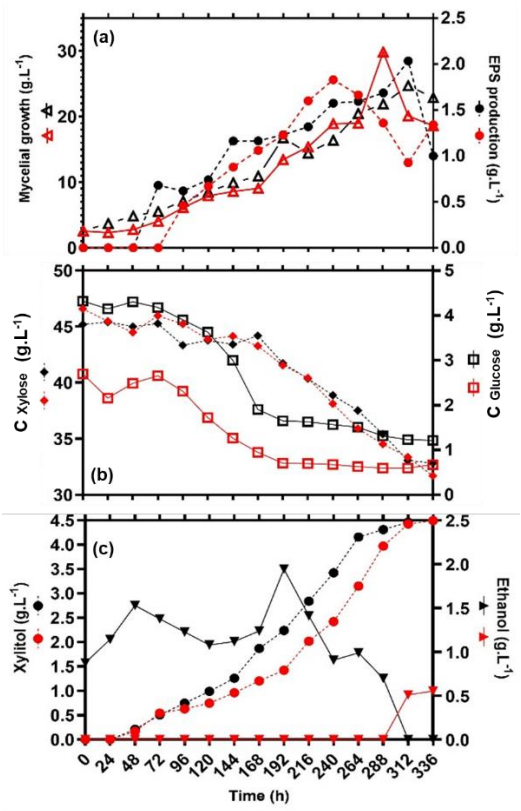

297

298 **Fig. 4.** Experimental data of EPS production and mycelial growth (a), xylose/glucose concentrations (b),

299 xylitol and ethanol production (c) by S. commune 227E.32 grown in an stirred-tank reactor.

300 **Table 1**. Mycelium growth and EPS production of *Schizophyllum commune* 227E.32 in a STR.

	X (g.L^{-1})	**P (g.L^{-1})**	**Y $_{P/X}$ (g/g)**	**Y $_{P/S}$ (g/g)**	**Y $_{X/S}$ (g/g)**
Experiment 1 - 10% of pre-inoculum	29.83	1.82	0.061	0.90	14.21
Experiment 2 - 20% of pre-inoculum	24.70	2.03	0.082	0.66	8.00

Legend: X – maximum mycelium growth ($g.L^{-1}$); P – maximum EPS production ($g.L^{-1}$); Y P/X – specific product yield (g EPS.g $mycelium^{-1}$); Y P/S – product yield (g EPS.g $sugar^{-1}$); Y X/S – mycelium yield (g mycelium/g $sugar^{-1}$).

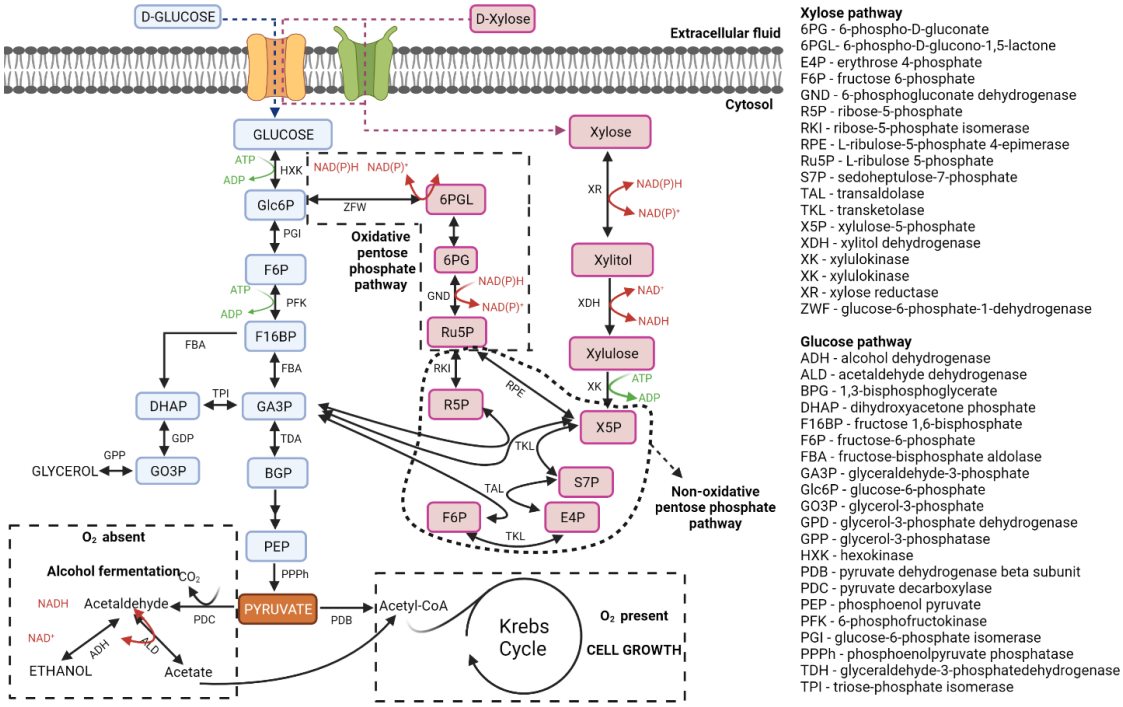

Fig. 5. *S. commune* 227E.32 glucose and xylose metabolic pathways. This metabolic pathway was elaborated based on the publications of Chu and Lee (2007); Lee and collaborators (2020).

3.4 EPS purification and characterization

The EPS fraction was partially soluble in water, and some insoluble parts remaining in suspension were notable. For this reason, a sequence of purification steps was performed (Fig. 1). Four fractions resulted from purification: EXO-I, EXO-ME, EXO-SMR and EXO-MR "gel". Their monosaccharide compositions are detailed in Table 2.

Table 1. Monosaccharide composition of polysaccharide fractions resulting from *S. commune* 227E.32 exopolysaccharide purification processes.

FRACTION	Mass (mg)	Monosaccharide composition (%)[a]					
		Fuc[b]	Ara[b]	Xyl[b]	Man[b]	Glc[b]	Gal[b]
EXO	200.0	-	1.4	12.7	3.8	79.2	2.9
EXO-I	40.0	1.3	0.7	16.0	26.5	67.4	2.5
EXO-ME	18.8	-	7.6	86.4	Tr.[c]	4.1	1.9

EXO-SMR	13.0	-	-	2.0	1.7	90.4	5.9
EXO-MR gel	124.0	-	-	-	-	100.0	-

[a] Analyzed in GC-MS (HP5-MS column) after total acid hydrolysis, $NaBH_4$ reduction and acetylation.
[b] Ara: arabinose; Xyl: xylose; Man: mannose; Glc: glucose and Gal: galactose. [c] Tr = traces.

The sequence of purification steps resulted in a apparent gel-like fraction, fully soluble in water, named EXO-MR "gel". According to GC-MS chromatograms its monosaccharide composition presented 100% glucose content corresponding to 62% of the crude material.

Then, EXO-MR "gel" could be identified as the well-known schizophyllan (β-(1→3)(1→6)-glucan) by NMR analysis (Fig. 6). ^{13}C NMR and HSQC-edit (Heteronuclear Single Quantum Coherence) were performed in Me_2SO-d_6 to assign the signals (Fig 6 a,b). Chemical assignments were pointed and described according to previous data (Kono et al., 2017a, 2017b). Four sets of ^{1}H-^{13}C spin correlation were noticed. It consists of six carbon atoms and seven protons of the glucose residue units, which can be attributed to the repeating units of schizophyllan (Kono et al., 2017a). This work identified glucose residues as **A**, **B**, **B'** and **C**. As shown in Figures 6a and 6b, all anomeric ^{1}H and the ^{13}C resonances of **B** and **B'** were completely overlapped, while **A** and **C** ^{13}C resonances of the glucose residues appeared separate. The chemical shifts of the schizophyllan ^{1}H and ^{13}C resonances were determined by the HSQC-edit spectrum, which details on the correlations between direct-coupling ^{1}H and ^{13}C spin pairs (Table S2, supplementary material. The RMN spectra were identical to the one reported by Kono and collaborators (2017a) with a β-D-Glc*p* (1→3) main chain, partially substituted at O-6 by nonreducing ends of β-D-Glc*p*, according to the structure proposed in the Figure 6c. Comparing the spectra obtained by this work, it was possible to suggest that the purified fraction EXO-MR "gel" showed a similarity to the schizophyllan produced by *Schizophyllum commune* strains. The methylation data agrees with those of NMR, being

observed only non-reducing terminals of Glcp (2,3,4,6-Me4-Glc) and Glcp 3-*O*-units (2,4,6-Me3- Glc) and 3,6-di-*O*-substituted (2,4-Me2-Glc), in a molar ratio of 1:2:1, respectively. The C/H assignments obtained are described in Table S2, supplementary material.

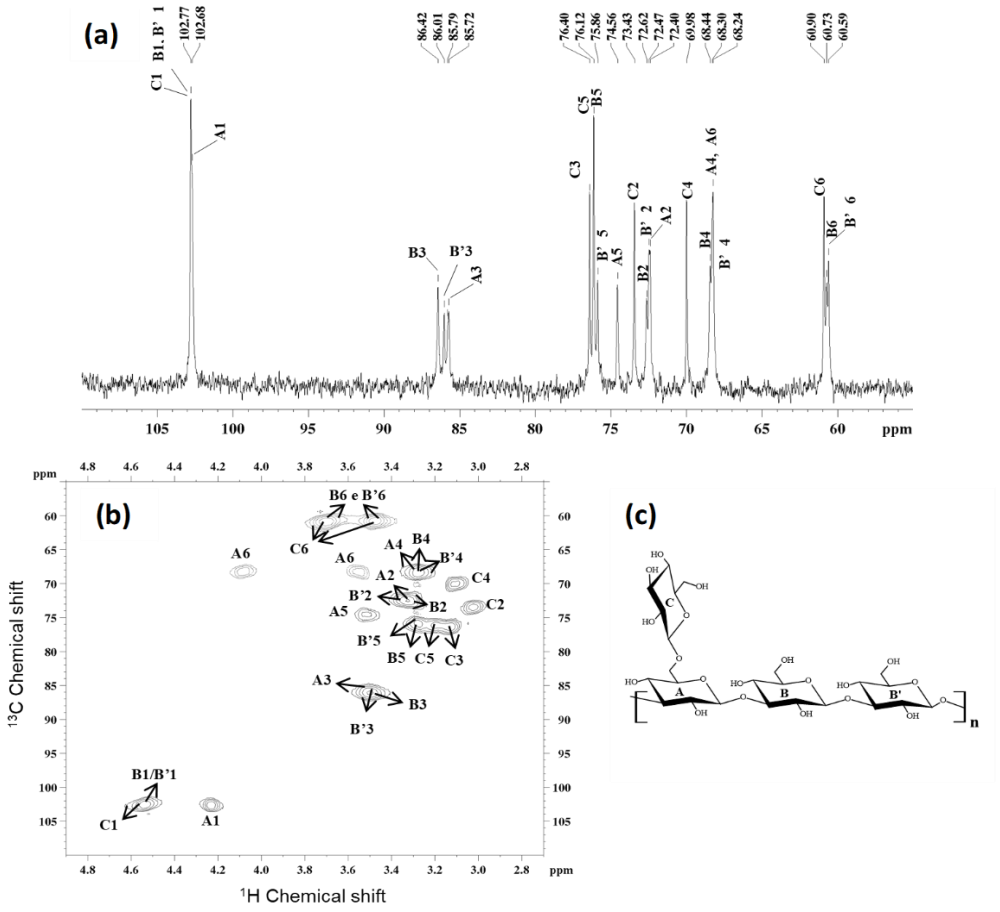

Fig. 6. ^{13}C NMR (Nuclear magnetic resonance) spectra (a) and HSQC-edit (b) (Heteronuclear Single Quantum Coherence) in Me_2SO-d_6 of β-(1→3)(1→6)-glucan produced by *S. commune* 227E.32 in STR (chemical shifts are expressed in δ, ppm); (c) proposed structure of β-(1→3) with substitution at O-6 by non-reducing β-Gl*cp* terminals.

Having established that the purified EPS has a primary structure of a β-D-Gl*cp* (1→3) main chain comb like branched with β-D-Gl*cp* (1→6) on every third backbone residue, we proceeded with characterization of macromolecular properties of the isolated schizophyllan by determination of M_w and ultrastructure imaging by AFM. The weight average molar mass determined by GPC/SEC analysis were 1.5 x 10^6 g.mol^{-1} and 1.1 x

352 10^6 g.mol^{-1} for the EPS obtained by the shaken flask and the STR processes, respectively.
353 Differences in M_w were expected since the two processes of production (shaken flasks
354 and STR) are very different, mainly in terms of aeration and stirring speed. The AFM
355 topographs (Fig. 7) reveal semiflexible structures distinctively appearing from a clear,
356 homogeneous background. This latter of feature evident in the topographs indicate an
357 efficient purification process. It is widespread that proteins from the fermentation process
358 remain bound to the polysaccharide in the ethanolic precipitation step. However, a very
359 clear background with no evidence of molecules remaining from the purification process
360 was observed. The semiflexible macromolecular structures appearing in the topographs
361 are similar to that reported for triplex structures of β-(1→3) glucans (Yanaki et al., 1983)
362 and different in appearance from dispersed single chains of β-(1→3) glucans obtained by
363 introducing charged groups in the side-chains and thereby induce triple helical
364 dissociation be electrostatic repulsion (Stokke et al., 2001). The adoption of the triple
365 helical state in the present EPS sample with an M_w of 1.1 x10^6 g.mol^{-1} is also consistent
366 with the molar mass dependence on the transition from the dispersed chains to triple
367 helical state reported to occur at about 4 x 10^3 g.mol^{-1} (Yanaki et al., 1983). The AFM
368 topographs obtained for preparation starting from an EPS concentration of 1 µg/mL, (Fig.
369 7a) indicate well dispersed molecules with different chain lengths reflecting
370 polydispersity of the sample. Increasing the concentration to a higher concentration (20
371 µg/mL) yields an appearance where the ends of the individual chains are not so clearly
372 distinguishable, and where the tendency to overlap does not result in lateral aggregation
373 of the chain segments.

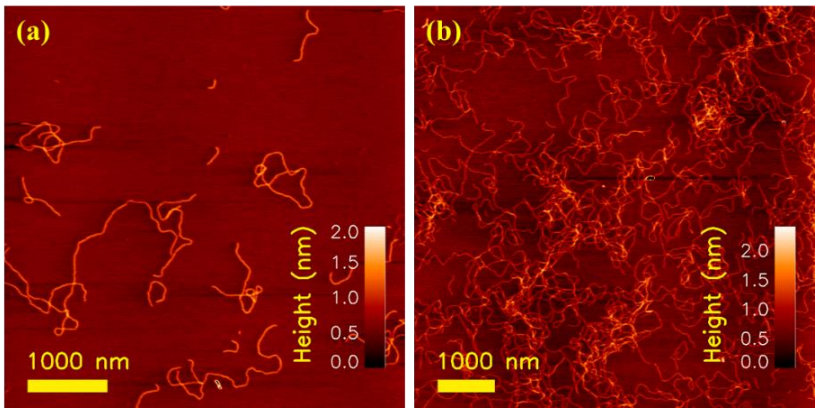

Fig. 7. Tapping mode AFM height topographs of purified schizophyllan produced from *S. commune* 227E.32 in STR process prepared for AFM characterization at (a) 1 µg.mL^{-1}, (b) 20 µg.mL^{-1}. The scan areas of the topographs were 5 x 5µm in (a) and 7 x 7µm in (b). These topographs were obtained for the schizophyllan with M_w = 1.1 x 10^6 g.mol^{-1}.

4. Conclusions

The significant contribution of the present study was to show the metabolic flexibility of the wild-type strain of *S. commune* 227E.32 to metabolize glucose and xylose as carbon sources to produce an exopolysaccharide, schizophyllan. This conclusion was based on experimental observations, such as xylitol and ethanol production by the strain, monitoring consumption of the carbon sources, and corroborated by analysis of pentose metabolic pathway enzymes for *Schizophyllum* strains.

Acknowledgements

This study was supported by University of Caxias do Sul (UCS) and financed in part by the Coordenação de Aperfeiçoamento de Pessoal de Nível Superior – Brasil (CAPES). The authors acknowledge the members of Dr. Antônio Gilberto Ferreira research's group from the Federal University of São Carlos for supporting the NMR experiments.

References

Carbonero, E. R., Ruthes, A. C., Freitas, C. S., Utrilla, P., Gálvez, J., Silva, E. V. da, Sassaki, G. L., Gorin, P. A. J., & Iacomini, M. (2012). Chemical and biological properties of a highly branched β-glucan from edible mushroom *Pleurotus sajor-caju*. *Carbohydrate Polymers*, *90*(2), 814–819. https://doi.org/10.1016/J.CARBPOL.2012.06.005

Chu, B. C. H., & Lee, H. (2007). Genetic improvement of *Saccharomyces cerevisiae* for xylose fermentation. In *Biotechnology Advances* (Vol. 25, Issue 5, pp. 425–441). https://doi.org/10.1016/j.biotechadv.2007.04.001

Ciucanu, I., & Kerek, F. (1984). A Simple and rapid method for the permethylation of carbohydrates. https://doi.org/0008-6215/84/$ 03.00

Du, B., Yang, Y., Bian, Z., & Xu, B. (2017). Molecular weight and helix conformation determine intestinal anti-inflammatory effects of exopolysaccharide from *Schizophyllum commune*. *Carbohydrate Polymers*, *172*, 68–77. https://doi.org/10.1016/j.carbpol.2017.05.032

Falcone, M., & Marques, A. B. (1965). Estudo sobre condições de hidrólise pelo ácido clorídrico na dosagem de açúcares redutores totais. *Technol. Ali. Beb.*, *4*, 24–30.

Fariña, J. I., Siñeriz, F., Molina, O. E., & Perotti, N. I. (2001). Isolation and physicochemical characterization of soluble scleroglucan from Sclerotium rolfsii. Rheological properties, molecular weight and conformational characteristics. *Carbohydrate Polymers*. https://doi.org/10.1016/S0144-8617(00)00189-2

García-Ochoa, F., Castro, E. G., & Santos, V. E. (2000). Oxygen transfer and uptake rates during xanthan gum production. https://doi.org/0141-0229/00/$

Horisawa, S., Ando, H., Ariga, O., & Sakuma, Y. (2015). Direct ethanol production from cellulosic materials by consolidated biological processing using the wood rot fungus *Schizophyllum commune*. *Bioresource Technology*, *197*, 37–41. https://doi.org/10.1016/j.biortech.2015.08.031

Jamshidian, H., Shojaosadati, S. A., Vilaplana, F., Mousavi, S. M., & Soudi, M. R. (2016). Characterization and optimization of schizophyllan production from date

syrup. *International Journal of Biological Macromolecules*, *92*, 484–493. https://doi.org/10.1016/j.ijbiomac.2016.07.059

Kim, H., Lee, S., & Ki, C. S. (2021). Modular formation of hyaluronic acid/β-glucan hybrid nanogels for topical dermal delivery targeting skin dendritic cells. *Carbohydrate Polymers*, *252*. https://doi.org/10.1016/j.carbpol.2020.117132

Kono, H., Kondo, N., Hirabayashi, K., Ogata, M., Totani, K., Ikematsu, S., & Osada, M. (2017a). NMR spectroscopic structural characterization of a water-soluble β-(1 → 3, 1 → 6)-glucan from Aureobasidium pullulans. *Carbohydrate Polymers*, *174*, 876–886. https://doi.org/10.1016/j.carbpol.2017.07.018

Kono, H., Kondo, N., Hirabayashi, K., Ogata, M., Totani, K., Ikematsu, S., & Osada, M. (2017b). Two-dimensional NMR data of a water-soluble β-(1→3, 1→6)-glucan from Aureobasidium pullulans and schizophyllan from Schizophyllum commune. *Data in Brief*, *15*, 382–388. https://doi.org/10.1016/J.DIB.2017.09.067

Leathers, T. D., Nunnally, M. S., Stanley, A. M., & Rich, J. O. (2016). Utilization of corn fiber for production of schizophyllan. *Biomass and Bioenergy*, *95*, 132–136. https://doi.org/10.1016/j.biombioe.2016.10.001

Lee, J. W., Kwak, S., Liu, J. J., Yu, S., Yun, E. J., Kim, D. H., Liu, C., Kim, K. H., & Jin, Y. S. (2020). Enhanced 2′-Fucosyllactose production by engineered Saccharomyces cerevisiae using xylose as a co-substrate. *Metabolic Engineering*, *62*, 322–329. https://doi.org/10.1016/j.ymben.2020.10.003

Liu, Z., Jiao, Y., Lu, H., Shu, X., & Chen, Q. (2019). Chemical characterization, antioxidant properties and anticancer activity of exopolysaccharides from Floccularia luteovirens. *Carbohydrate Polymers*. https://doi.org/10.1016/j.carbpol.2019.115432

Mandels, M., & Reese, E. T. (1960). Induction of cellulase in fungi by cellobiose. *Journal of Bacteriology*, *79*(Cx), 816–826. http://www.ncbi.nlm.nih.gov/pubmed/14420566%0Ahttp://www.pubmedcentral.nih.gov/articlerender.fcgi?artid=PMC278786

Matsushika, A., Inoue, H., Kodaki, T., & Sawayama, S. (2009). Ethanol production from xylose in engineered Saccharomyces cerevisiae strains: Current state and

perspectives. In *Applied Microbiology and Biotechnology* (Vol. 84, Issue 1, pp. 37–53). https://doi.org/10.1007/s00253-009-2101-x

Nguyen, H. S. H., Kaspereit, M., & Sainio, T. (2021). Intermittent recycle-integrated reactor-separator for production of well-defined non-digestible oligosaccharides from oat β-glucan. *Chemical Engineering Journal*, *410*, 128352. https://doi.org/10.1016/j.cej.2020.128352

Rekik, H., Zaraî Jaouadi, N., Bouacem, K., Zenati, B., Kourdali, S., Badis, A., Annane, R., Bouanane-Darenfed, A., Bejar, S., & Jaouadi, B. (2019). Physical and enzymatic properties of a new manganese peroxidase from the white-rot fungus Trametes pubescens strain i8 for lignin biodegradation and textile-dyes biodecolorization. *International Journal of Biological Macromolecules*, *125*, 514–525. https://doi.org/10.1016/j.ijbiomac.2018.12.053

Ruiz-Herrera, J., & Ortiz-Castellanos, L. (2019). Cell wall glucans of fungi. A review. In *Cell Surface* (Vol. 5). Elsevier B.V. https://doi.org/10.1016/j.tcsw.2019.100022

Safaee-Ardakani, M. R., Hatamian-Zarmi, A., Sadat, S. M., Mokhtari-Hosseini, Z. B., Ebrahimi-Hosseinzadeh, B., Rashidiani, J., & Kooshki, H. (2019). Electrospun Schizophyllan/polyvinyl alcohol blend nanofibrous scaffold as potential wound healing. *International Journal of Biological Macromolecules*, *127*, 27–38. https://doi.org/10.1016/j.ijbiomac.2018.12.256

Schneider, W. D. H., Fontana, R. C., Baudel, H. M., de Siqueira, F. G., Rencoret, J., Gutiérrez, A., de Eugenio, L. I., Prieto, A., Martínez, M. J., Martínez, Á. T., Dillon, A. J. P., & Camassola, M. (2020). Lignin degradation and detoxification of eucalyptus wastes by on-site manufacturing fungal enzymes to enhance second-generation ethanol yield. *Applied Energy*, *262*. https://doi.org/10.1016/j.apenergy.2020.114493

Shoaib, M., Quadri, S. M. R., Wani, O. B., Bobicki, E., Garrido, G. I., Elkamel, A., & Abdala, A. (2020). Adsorption of enhanced oil recovery polymer, schizophyllan, over carbonate minerals. *Carbohydrate Polymers*, *240*. https://doi.org/10.1016/j.carbpol.2020.116263

Shu, C. H., & Hsu, H. J. (2011). Production of schizophyllan glucan by Schizophyllum commune ATCC 38548 from detoxificated hydrolysate of rice hull. *Journal of the*

Taiwan Institute of Chemical Engineers, *42*(3), 387–393. https://doi.org/10.1016/j.jtice.2010.08.009

Singh, M. K., Kumar, M., & Thakur, I. S. (2017). Proteomic characterization and schizophyllan production by Schizophyllum commune ISTL04 cultured on Leucaena leucocephala wood under submerged fermentation. *Bioresource Technology*, *236*, 29–36. https://doi.org/10.1016/j.biortech.2017.03.170

Smirnou, D., Knotek, P., Nesporova, K., Smejkalova, D., Pavlik, V., Franke, L., & Velebny, V. (2017). Ultrasound-assisted production of highly-purified β-glucan schizophyllan and characterization of its immune properties. *Process Biochemistry*, *58*, 313–319. https://doi.org/10.1016/j.procbio.2017.04.016

Stokke, B. T., Falch, B. H., & Dentini, M. (2001). Macromolecular Triplex Zipping Observed in Derivatives of Fungal (1 3 3)-D-Glucan by Electron and Atomic Force Microscopy. In *NRC) Biopolymers* (Vol. 58).

Sutivisedsak, N., Leathers, T. D., & Price, N. P. J. (2013). Production of schizophyllan from distiller's dried grains with solubles by diverse strains of Schizophyllum commune. *SpringerPlus*, *2*(1), 1–6. https://doi.org/10.1186/2193-1801-2-476

Tyler, J. M., & Branton, D. (1980). Rotary shadowing of extended molecules dried from glycerol. *Journal of Ultrastructure Research*, *71*(2), 95–102. https://doi.org/10.1016/S0022-5320(80)90098-2

Utama, G. L., Dio, C., Sulistiyo, J., Yee Chye, F., Lembong, E., Cahyana, Y., Kumar Verma, D., Thakur, M., Patel, A. R., & Singh, S. (2021). Evaluating comparative β-glucan production aptitude of Saccharomyces cerevisiae, Aspergillus oryzae, Xanthomonas campestris, and Bacillus natto. *Saudi Journal of Biological Sciences*. https://doi.org/10.1016/J.SJBS.2021.07.051

Viñarta, S. C., François, N. J., Daraio, M. E., Figueroa, L. I. C., & Fariña, J. I. (2007). Sclerotium rolfsii scleroglucan: The promising behavior of a natural polysaccharide as a drug delivery vehicle, suspension stabilizer and emulsifier. *International Journal of Biological Macromolecules*, *41*(3), 314–323. https://doi.org/10.1016/J.IJBIOMAC.2007.04.001

Wolfrom, M. L., & Thompsom, A. (1963). *Acetylation. Methods in Carbohydrate Chemistry* (211th ed., Vol. 2b).

513 Wolfrom, M. L., & Thompson, A. (1963). *A reduction with sodium borohydride". Methods in Carbohydrate Chemistry* (65th ed., Vol. 2a).

515 Wu, Y., Choi, M. H., Li, J., Yang, H., & Shin, H. J. (2016). Mushroom cosmetics: The present and future. In *Cosmetics* (Vol. 3, Issue 3). MDPI AG. https://doi.org/10.3390/cosmetics3030022

518 Xu, H., Zou, S., Xu, X., & Zhang, L. (2016). Anti-Tumor effect of β-glucan from Lentinus edodes and the underlying mechanism. *Scientific Reports*, *6*. https://doi.org/10.1038/srep28802

521 Yanaki, T., Ito, W., Tabata, K., Kojima, T., Norisuye, T., Takano, N., & Fujita, H. (1983). Correlation between the antitumor activity of a polysaccharide schizophyllan and its triple-helical conformation in dilute aqueous solution. *Biophysical Chemistry*, *17*(4), 337–342. https://doi.org/10.1016/0301-4622(83)80018-0

525 Zhang, Y., Kong, H., Fang, Y., Nishinari, K., & Phillips, G. O. (2013). Schizophyllan: A review on its structure, properties, bioactivities and recent developments. *Bioactive Carbohydrates and Dietary Fibre*, *1*(1), 53–71. https://doi.org/10.1016/J.BCDF.2013.01.002

529 Zhang, Y., Zeng, Y., Men, Y., Zhang, J., Liu, H., & Sun, Y. (2018). Structural characterization and immunomodulatory activity of exopolysaccharides from submerged culture of Auricularia auricula-judae. *International Journal of Biological Macromolecules*, *115*, 978–984. https://doi.org/10.1016/J.IJBIOMAC.2018.04.145

533 Zhong, K., Tong, L., Liu, L., Zhou, X., Liu, X., Zhang, Q., & Zhou, S. (2015). Immunoregulatory and antitumor activity of schizophyllan under ultrasonic treatment. *International Journal of Biological Macromolecules*, *80*, 302–308. https://doi.org/10.1016/J.IJBIOMAC.2015.06.052

537 Zhu, F., Du, B., & Xu, B. (2016). A critical review on production and industrial applications of beta-glucans. In *Food Hydrocolloids*. https://doi.org/10.1016/j.foodhyd.2015.07.003

540